

To appear in *Engineering Optimization*
Vol. 00, No. 00, Month 20XX, 1–27

Mooring System Design Optimization Using a Surrogate Assisted Multi-Objective Genetic Algorithm

Ajit C. Pillai^{a*} Philipp R. Thies^a and Lars Johanning^a

^a*Renewable Energy Group, College of Engineering, Mathematics, and Physical Sciences,
University of Exeter, Penryn, United Kingdom*

(v3.0 draft July 2018)

This article presents a novel framework for the multi-objective optimization of offshore renewable energy mooring systems using a random forest based surrogate model coupled to a genetic algorithm. This framework is demonstrated for the optimization of the mooring system for a floating offshore wind turbine highlighting how this approach can aid in the strategic design decision making for real-world problems faced by the offshore renewable energy sector. This framework utilizes validated numerical models of the mooring system to train a surrogate model, which leads to a computationally efficient optimization routine, allowing the search space to be more thoroughly searched. Minimizing both the cost and cumulative fatigue damage of the mooring system, this framework presents a range of optimal solutions characterizing how design changes impact the trade-off between these two competing objectives.

Keywords: offshore renewable energy; mooring system design; surrogate modelling; multi-objective optimization; reliability based design optimization

1. Introduction

As the offshore renewable energy sector progresses, it has become increasingly important to ensure that designs simultaneously generate the desired energy, survive in their energetic surroundings for their full lifetime, and remain cost effective. In the quest to satisfy these competing objectives, optimization techniques are now deployed in the design process to identify new design concepts while also aiding the system designer in strategic design decision-making. With progressively more offshore renewable energy devices exploring floating solutions, mooring systems have become one of the key sub-systems which impacts both the survivability of the device and its costs (Weller et al. 2015; Thomsen et al. 2018). However, due to the computational time associated with the simulation of mooring systems it is not yet commonplace to deploy optimization algorithms in the design cycle. Without the use of numerical optimization methods, the design of mooring systems is limited to an iterative engineering design approach based on experience and engineering judgement. This often leads to innovative mooring designs not being considered, and the deployment of sub-optimal mooring designs (Johanning, Smith, and Wolfram 2006). In order to implement optimization techniques in complex engineering design problems, surrogate modelling, the use of simpler low fidelity models which approximate the high fidelity results at a lower computation cost, have emerged as an important technique to improve the computational time associated with these

*Corresponding author. Email: a.pillai@exeter.ac.uk

20 optimization schemes (Won and Ray 2005; Voutchkov and Keane 2006; Jin 2011).

21 The field of mooring optimization is a relatively nascent field which explores the optimal
22 selection of mooring line materials, lengths, and diameters in order to elicit a desired
23 response or minimize the cost associated with a floating system. As mooring systems
24 represent an important component of offshore renewable energy devices which impact
25 not only the motion dynamics of the device, and therefore how it interacts with the
26 resource from which it is extracting energy, but also affects the cost of the overall system
27 and governs the lifetime of the device (Weller et al. 2015). In the design of mooring
28 systems, it is therefore common to select designs which minimize the cost or excursions
29 subject to constraints on the tension in the lines, and the fatigue in the mooring system.
30 Given this complex set of design considerations, an optimization approach and multi-
31 objective optimization in particular would be appropriate in order to characterize the
32 trade-offs between the competing design objectives and better inform decision making.

33 Existing work in the optimal design of mooring systems has explored the geometry
34 optimization of the mooring system using a genetic algorithm to minimize the response
35 of the moored vessels and platforms (Carbono, Menezes, and Martha 2005; Shafieefar
36 and Rezvani 2007; Ryu et al. 2007; da Fonesca Monteiro et al. 2016; Ryu et al. 2016).
37 However, as these studies have focused on vessels and platforms, these may not be the
38 most appropriate optimizer objectives for an offshore renewable energy device. The recent
39 work by Thomsen et al. (2018) has specifically explored the optimization of mooring
40 systems for a wave energy converter considering the minimization of cost, however, the
41 use of single objective optimization does not fully capture the complexity of the design
42 problem. Offshore renewable energy devices must be both cost effective and achieve
43 a specific device response in order to effectively harness the energy sources. Work by
44 the authors has, therefore, explored multi-objective optimization of mooring systems for
45 renewable energy platforms in order to highlight potential design trade-offs between the
46 competing objectives that a device designer would face thereby offering information to
47 allow the system designers to make more informed decisions (Pillai, Thies, and Johanning
48 2017, 2018b).

49 The assessment of mooring system designs is generally achieved through finite element
50 analysis software operating in either the time domain or frequency domain (Davidson
51 and Ringwood 2017). Time domain finite element models are capable of capturing the
52 dynamic behaviour of the mooring lines and therefore play an important role in the
53 design process. However, in order to effectively assess the response of the mooring be-
54 haviour, simulations must be executed for each operating condition and for sufficiently
55 long simulations in order to adequately capture the dynamic behaviour during any oper-
56 ational sea state (Thomsen, Eskilsson, and Ferri 2017). Previous work by the authors has
57 highlighted the importance of utilizing time domain simulations when designing mooring
58 systems for renewable energy devices as these devices are characterized by more dynamic
59 motion than vessels or platforms, therefore, requiring a simulation domain which can cap-
60 ture these dynamic effects and the impact that this has on the fatigue and design life of
61 the mooring system. Mooring system optimization without surrogate models (Carbono,
62 Menezes, and Martha 2005; Shafieefar and Rezvani 2007; Ryu et al. 2007; da Fonesca
63 Monteiro et al. 2016; Ryu et al. 2016) tend to rely on frequency domain simulations
64 which are significantly quicker and less computationally demanding than their time do-
65 main counterparts. Frequency domain methods, however, are not as effective in capturing
66 the dynamic motion and loading of mooring systems which may play an important role in
67 selecting appropriate mooring designs for offshore renewable energy applications (Kwan
68 and Bruen 1991; Brown and Mavrakos 1999; Pillai, Thies, and Johanning 2018a).

69 For many optimization problems, the true objective function(s) are computationally
70 costly. An effective approach to resolve this is to use a simpler objective function, a *sur-*
71 *rogate*, which is correlated to the true objective, but computationally less expensive (For-

72 rester, Sóbester, and Keane 2008). Surrogate modelling as a general term includes any
73 model which substitutes for a high fidelity model in order to reduce computational time.
74 These models can therefore attempt to model the underlying science with less detail or
75 can be statistical models built from results using the full model (Forrester, Sóbester,
76 and Keane 2007). Traditional forms of surrogate models include decision trees, support
77 vector machines, radial basis functions, and artificial neural networks, however, there
78 are also now many variations and hybrid approaches (Hastie, Tibshirani, and Friedman
79 2009; Forrester, Sóbester, and Keane 2008). Recent developments in the field of surrogate
80 modelling in the context of optimization has explored the use of ensembles of surrogates
81 to better define and characterize the search space (Forrester and Keane 2009; Forrester,
82 Sóbester, and Keane 2007; Chugh et al. 2018; Shankar Bhattacharjee, Kumar Singh, and
83 Ray 2016). Previous work in this field has focused on the development of generalized
84 strategies which are relevant to a wide range of engineering problems, while the focus
85 of the present paper is to demonstrate a specific methodology suitable to the mooring
86 system design and optimization problem. The present work, therefore, focuses on the
87 introduction and demonstration of the applicability of a specific methodology for this
88 specific problem.

89 Surrogate models built for the assessment of the motions of a moored structure and the
90 tensions in the mooring lines has generally made use of artificial neural networks (de Pina
91 et al. 2013, 2016; Sidarta et al. 2017). The use of surrogate models for mooring system
92 assessment, has, however, not been undertaken in the context of optimizing the mooring
93 system.

94 This paper bridges these two areas of research implementing both a genetic algorithm
95 for the geometry optimization of the mooring system of an offshore renewable energy
96 platform while utilizing a surrogate model built using a machine learning technique
97 in order to reduce the computational complexity of the optimizer evaluation function
98 through a functional approximation architecture. The developed framework represents
99 a pragmatic approach to the design of mooring systems offering a system designer the
100 potential to make more informed decisions regarding the design of the mooring system.
101 Though the optimization and surrogate models deployed are not on their own novel, their
102 integration into a unified framework for the present mooring system design framework
103 represents a novel implementation which is shown to aid the design process and marks
104 an improvement on the present standard approaches.

105 In the design of mooring systems there are several objectives which are often consid-
106 ered including the cost of the mooring system, the tension in the lines relative to the
107 minimum breaking load (MBL), the excursions of the floating body, or the cumulative
108 fatigue damage. For the presented case study, the optimization routine seeks to minimize
109 the cumulative lifetime fatigue damage in the mooring system and the material cost of
110 the mooring system. These have been selected as they represent two important design
111 criteria for mooring systems and especially for offshore renewable energy developers. Due
112 to increasing challenges in many-objective optimization, the present implementation is
113 as a bi-objective problem, though extensions including further objectives can be explored
114 within the framework in the future in order to simultaneously consider additional objec-
115 tives during the design process.

116 2. Mooring System Optimization Problem

117 The problem addressed in the present article explores the geometry optimization of
118 a mooring system for an offshore renewable energy device. Offshore renewable energy
119 devices extract energy from natural fluxes which cause some device motion relative to
120 this natural flux, be it the blades of a wind turbine relative to the wind, a tidal turbine's

121 rotor relative to the tidal current, or a wave energy device’s active surface relative to
 122 the sea surface elevation. As a result of this, floating renewable energy devices, must
 123 ensure that their mooring systems are designed achieving the desired behaviour while at
 124 the same time not adversely impacting the reliability or cost of the overall system. The
 125 optimal design of mooring systems must therefore consider the site at which a device
 126 is being deployed, the specific device characteristics, the mooring system itself, and the
 127 interactions between these elements.

128 For each of the mooring lines considered in the system, the optimization routine selects
 129 the position of the mooring line anchor, the length of the mooring line, the material of
 130 each section of the mooring line, and the diameter of each section of the mooring line.
 131 These decision variables are given in table 1. The optimization routine does not explicitly
 132 select the number of mooring lines, but takes this as an input.

Table 1.: Description of Decision Variables

Variable	Description	Variable Type
$x_{l,i}$	length of section i of line l	Continuous
$y_{l,i}$	construction of section i of line l	Integer
α_l	anchor horizontal position for line l	Continuous
θ_l	anchor angle for line l	Continuous

133 Though the mooring system is defined using only a few variables for each line, this
 134 formulation is efficient in capturing the elements of interest to a mooring designer and can
 135 be used to characterize the mooring system for any floating body. In the present work,
 136 each line has been limited to consisting of maximum of three sections which can differ in
 137 diameter, material, or both. This limit has been selected in part as this represents the
 138 maximum number of sections often utilized for offshore renewable energy devices, and it
 139 allows a significant degree of flexibility to the optimization process. Given the flexibility
 140 of the framework, should a designer wish to consider a greater degree of flexibility in the
 141 designs then additional sections can easily be considered.

142 While the variables describing the section lengths and anchor position are continuous
 143 variables, the line type is a categorical representing which of the predefined line types is
 144 to be deployed. A detailed description of the constraints, and restrictions on the decision
 145 variables follows in section 2.3.

146 2.1 *Cumulative Fatigue Damage*

147 Engineering design must consider different failure modes in order to ensure that the
 148 design is fit for purpose. This includes the ultimate limit state (ULS) which considers
 149 the maximum extreme loads that the system must withstand, as well as the fatigue limit
 150 state (FLS) which considers the possible failure as a result of repeated cyclic loading
 151 at levels below the ULS (Schijve 2009). Offshore renewable energy devices seek to be
 152 deployed for a period up to 25 years which therefore requires reliable systems which can
 153 ensure device survival over this lifetime. The first objective explored in this optimization
 154 problem is therefore the fatigue damage in the mooring system. The fatigue damage is
 155 assessed using simulated tension time-series for each proposed mooring system for each
 156 of the anticipated sea states at the installation site. From this, rainflow counting of the
 157 tension cycles is done at each point along the lengths of the mooring lines.

158 Rainflow counting is a methodology used to evaluate fatigue damage for load cycles of
 159 varying amplitude. This method operates by identifying and counting the stress ranges
 160 corresponding to individual hysteresis loops. This is then used in combination with S-N

161 or T-N curves which define the number of stress (S-N) or tension (T-N) cycles at a specific
 162 amplitude required for the material to reach failure. The Palmgren-Miner rule, shown
 163 in eq. (1), allows the individual contribution of each stress cycle to be summed in order
 164 to compute the cumulative fatigue damage (Rychlik 1987; Amzallag et al. 1994; Schijve
 165 2009; Thies et al. 2014). The lifetime fatigue damage of the mooring lines is established
 166 by carrying out these calculations for each sea state that is expected at the site, and
 167 scaling the fatigue contributions based on the relative occurrence of the sea states over
 168 the operational lifetime of the device.

$$D(t) = \sum_{t_k < t} \frac{1}{N(S)} = \frac{1}{K} \sum_{t_k < t} (S)^\beta \quad (1)$$

169 where $D(t)$ is the fatigue damage, $N(S)$ is the number of cycles during time t , and S
 170 denotes the stress amplitudes established in the rainflow cycle count. The parameters K
 171 and β describe the fatigue properties of the material and are given by the S-N and T-N
 172 curves.

The cumulative fatigue damage, D_c is then given by:

$$D_c = \sum_{s \in \mathcal{S}} D_s \times \frac{T}{\tau_d} \times P(s) \quad (2)$$

173 where s represents a sea state from \mathcal{S} , the set of sea states which are simulated, T is
 174 the operational lifetime of the mooring system, τ_d is the simulation duration, and $P(s)$
 175 is the probability of occurrence associated with sea state s . For each mooring line, the
 176 cumulative fatigue is computed at each point along the mooring line in order to consider
 177 the possible failure anywhere along the line and not exclusively at the fairleads. Though
 178 the highest tensions are experienced at the fairleads, the fatigue damage may be higher
 179 elsewhere in the system and it is important to consider the possible failure at any position
 180 along the mooring lines.

181 The objective, the minimization of the cumulative fatigue damage is explicitly given
 182 in eq. (4a) in the full problem formulation.

183 2.2 Material Cost

184 As cost effective solutions are sought, the second objective explored in the mooring design
 185 problem is the minimization of the material cost of the mooring lines. This is computed as
 186 a sum over the mooring lines by multiplying the unit cost of each line type (combination of
 187 material and diameter i.e. MBL) with the length of the line type deployed in the mooring
 188 system. In this way, this metric does not include any consideration of the anchors, and
 189 in fact the time-domain simulations do not affect this objective. This objective, the
 190 material cost of the mooring system, is, however, necessary as it represents a key metric
 191 that developers must consider when designing and deploying their mooring systems. The
 192 mooring system cost is computed using eq. (3) and the objective is given in eq. (4b) in
 193 the problem formulation.

$$C_l = \sum_{l \in \mathcal{L}} \sum_{i=1}^{\varepsilon_m} c(y_{l,i}) \cdot x_{l,i} \quad (3)$$

194 2.3 Constraints

195 In order to accurately model the design problem it is important to include constraints
 196 which limit the search space to feasible solutions and represent the real engineering
 197 limitations on the decision variables. Since the decision variables include the line speci-
 198 fications for each line as well as the anchor positions for each line's anchor, the genome
 199 is a mixture of various types.

200 The anchors are defined to be no further than 2500 m away from the floating body, and
 201 anchor lines are set to be within 30° of the original orientation defined in the simulation
 202 model (eqs. (4c) and (4d)). Specific constraints on the anchor positions will be site and
 203 project specific and these values have been selected for the present case study to illustrate
 204 the capabilities of the tool. The minimization of the mooring line costs will naturally try
 205 to limit the mooring footprint by bringing anchors in closer to the floating body, so this
 206 upper limit acts to aid the convergence of the optimizer. It is important to note that the
 207 present coupling to OrcaFlex does not simulate or model the anchors or any dynamics
 208 at the anchoring point and they are assumed to be a fixed point to the seabed.

209 Equation (4e) defines the length of mooring line to be the sum of the line segments
 210 and constrains this to be greater than zero to ensure that a mooring line is present while
 211 eq. (4f) imposes a constraint that the length of a mooring line cannot exceed the sum
 212 of the water depth and the horizontal distance to the anchor in order to ensure that the
 213 mooring line is not unrealistically long. Equation (4g) limits the tension along the length
 214 of the mooring line such that the minimum breaking load (MBL) of the line type at every
 215 location of the line is not exceeded. This constraint can optionally include F_s as a safety
 216 factor. Equation (4h) ensures that the line type for each line segment of each mooring
 217 line is one of those considered in the implementation of the optimization problem. Finally
 218 eqs. (4i) and (4j) define a set of points along each mooring line that are in contact with
 219 seabed during the dynamic simulation and limits these to chain constructions.

220 2.4 Problem Formulation

221 Given the decision variables, objectives, and constraints as described above, the full
 222 optimization problem can be formulated as follows:

$$\min f_1(x) = \max \left(\sum_{s \in \mathcal{S}} (D_c(x_l, y_l, \alpha_l, \theta_l, s) \cdot P(s)) \right) \quad \forall l \in \mathcal{L} \quad (4a)$$

$$\min f_2(x) = \sum_{l \in \mathcal{L}} \sum_{i=1}^{\varepsilon_m} c(y_{l,i}) \cdot x_{l,i} \quad (4b)$$

$$\text{s.t. } \alpha_l \leq 2500 \quad \forall l \in \mathcal{L} \quad (4c)$$

$$\theta_l \leq \phi_l \pm 30^\circ \quad \forall l \in \mathcal{L} \quad (4d)$$

$$L_l = \sum_{i=0}^{\varepsilon_m} x_i \geq 0 \quad \forall l \in \mathcal{L} \quad (4e)$$

$$L_l = \sum_{i=0}^{\varepsilon_m} x_i \leq \alpha_l + h \quad \forall l \in \mathcal{L} \quad (4f)$$

$$t_{l,a} \leq MBL_{l,a} \times F_s \quad \forall l \in \mathcal{L}; \quad (4g)$$

$$\forall a \in]0, L_l];$$

$$\begin{aligned}
y_{l,a} &\in \mathcal{A} & \forall s \in \mathcal{S} \\
\mathcal{G}_l &= \{i | v_{l,a} \leq 0\} & \forall l \in \mathcal{L}; \quad (4h) \\
y_{l,i} &\in \mathcal{C} & \forall a \in]0, L_l]; \\
& & \forall l \in \mathcal{L}; \quad (4i) \\
& & \forall a \in]0, L_l] \\
& & \forall l \in \mathcal{L}; \quad (4j) \\
& & \forall i \in G_l
\end{aligned}$$

223 where f_1 is the first objective function representing the cumulative fatigue damage, f_2
224 is the cost objective, x_l is the decision variables for the section lengths of mooring line
225 l , y_l is the decision variables for the section constructions of mooring line l , α_l is the
226 decision variables for the horizontal distance between the platform and mooring line l 's
227 anchor, and θ_l is the decision variable for the angle between the platform and mooring
228 line l 's anchor. \mathcal{L} , \mathcal{S} , \mathcal{A} and \mathcal{C} are the sets representing all the mooring lines, the sea
229 states to examine, the available line constructions, and the line constructions which are
230 chain respectively. The remaining variables in the above formulation are: s a sea state
231 from the set of sea states, d the cumulative fatigue damage, $P(s)$ the probability of
232 occurrence for sea state s , $c(y_{l,i})$ the unit cost of a mooring line construction, ϕ_l the
233 initial orientation of mooring line l , $MBL_{l,a}$ the minimum breaking load at position a
234 along line l , F_s the factor of safety on the mooring line tensions, a a position along the
235 line, \mathcal{G}_l the set of nodes along each mooring line which are in contact with the seabed,
236 $v_{l,i}$ the minimum vertical distance between the seabed and node i along mooring line l
237 during the simulation, and h is the water depth.

238 In this formulation f_1 and f_2 can be evaluated using any relevant model, be it the full
239 dynamic simulations using OrcaFlex or the surrogate model detailed in section 3.2. In
240 this way, either method takes the same input features (i.e. the genome) and provides the
241 estimates of the cumulative fatigue damage and material cost (i.e. the output features).

242 3. Solution Approach

243 3.1 Process Overview

244 Optimization algorithms are methods which seek to identify the best possible solution
245 from those available. To do this, they make use of a search algorithm to explore the
246 possible decision variable values with respect to some objective functions (Burke and
247 Kendall 2013). For real-world problems, it is often challenging to accurately formulate
248 these evaluation functions such that the intra-relationships between the decision variables
249 are captured in a time-efficient manner (Jin 2005, 2011). To overcome this, optimization
250 of real-world problems can opt to replace the complex evaluation function with a simpler,
251 less expensive approximate model: a surrogate model. For these surrogate models to be
252 of use, they need to be able to capture the trends of the full evaluation function, so
253 that on a relative basis, the results of the surrogate optimization problem can inform the
254 original problem.

255 For the mooring optimization problem, the full time-domain simulations are run using
256 OrcaFlex, an industry standard software package for the time domain analysis of off-
257 shore structures. This software package is capable of modelling the tension in mooring
258 lines involving multiple members and materials, as well as the excursions of the moored
259 body (Thomsen, Eskilsson, and Ferri 2017). Using these full time domain simulations,

260 the surrogate model is built and trained, allowing proposed mooring systems during the
 261 optimization process to be assessed without the use of the full time-domain simulations.

262 The overall methodology is pictured in fig. 1 and makes use of both a multi-objective
 263 genetic algorithm, as well as the machine learning based surrogate model.

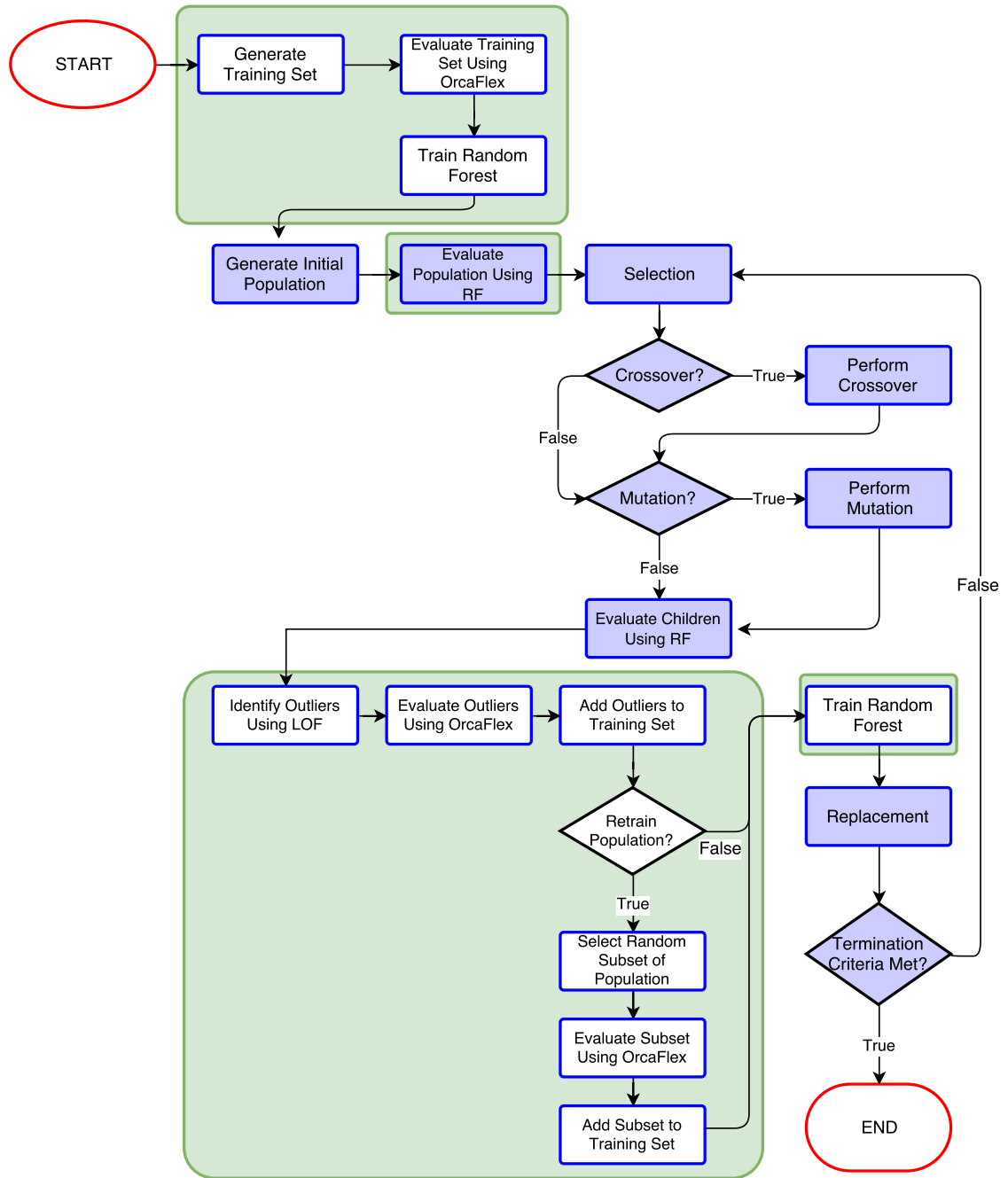


Figure 1.: Optimization process using a random forest surrogate model. The steps related to the surrogate model are highlighted in light green boxes, while the core steps of the genetic algorithm are shown in blue.

264 Machine learning techniques operate according to the principles illustrated in fig. 2 and
 265 are generally divided into *classification* and *regression* problems. In the case of a classi-
 266 fication problem, the output feature represents the classes that the input elements are
 267 grouped into, while for a regression problem the output features represent the quantities

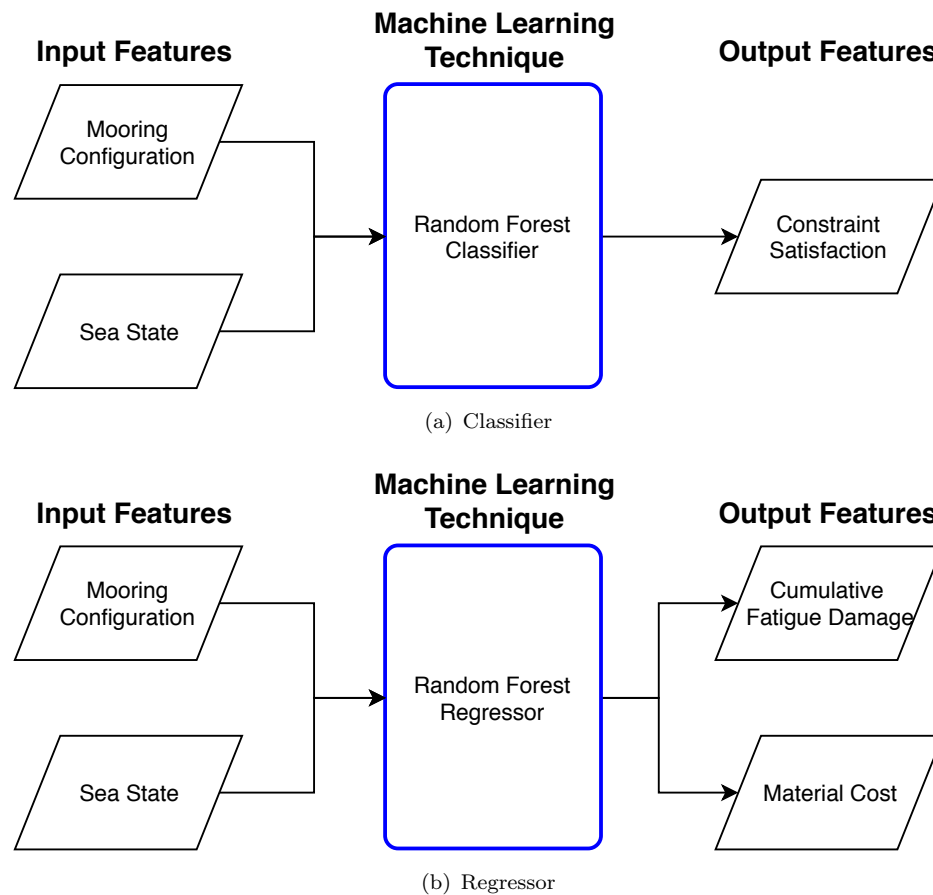


Figure 2.: Overview of machine learning estimators. Note that the number of input and output features are not necessarily related, though generally, there are fewer output features than there are input features. For the case of a classifier, the output features represent the classes to which each individual belongs while in the case of regression, the output features represent the values of interest.

268 of interest. Machine learning algorithms are often thought of as black boxes which seek to
 269 correlate the outputs features to the inputs features without simulating or modelling the
 270 underlying physics or engineering principles, but are purely statistical models. For any
 271 machine learning strategy, a training set, a set of inputs and outputs, is used to calibrate
 272 the black box model in order to build these statistical relationships. Machine learning
 273 techniques in general, therefore, work best with large training datasets from which the
 274 statistical correlations can be built. Furthermore, machine learning algorithms such as a
 275 neural network or random forest work best when they are *interpolating* between values
 276 on the training set rather than *extrapolating*. These algorithms therefore require that the
 277 training set cover the extent of the search space thereby allowing interpolation. Some
 278 machine learning algorithms such as random forests are capable of extrapolating output
 279 features, however, at a cost in accuracy.

280 In the present implementation, the input features to the machine learning technique
 281 are the decision variables of the optimization problem and the output features are the
 282 evaluated objective functions and the mooring system's satisfaction of the constraints.
 283 In this scheme, the surrogate model first estimates if the proposed solution will satisfy
 284 or violate the constraints, in the event that the model predicts that the constraints will
 285 be satisfied, the second phase of the surrogate estimates the objective function values.
 286 In effect, this surrogate model therefore, uses a classifier to determine the constraint

287 satisfaction component of the problem and then a regression method to determine the
 288 objective function values. OrcaFlex is therefore only used when training and retraining
 289 the learning algorithm and is no longer directly tied to the evaluation functions for the
 290 optimization. The full deployed procedure is shown in fig. 1 with the creation of the
 291 surrogate model highlighted in green. This new methodology follows five basic steps:

- 292 (1) Build a training set of possible mooring systems;
- 293 (2) Evaluate the training set using the original full time domain simulation-based eval-
 294 uation function;
- 295 (3) Use result from OrcaFlex model to train the surrogate model;
- 296 (4) Use surrogate model to perform optimization using NSGA-II;
- 297 (5) Retrain the surrogate as required.

298 A non-dominated sorting genetic algorithm II (NSGA-II) is used to optimize over
 299 multiple objective functions. This method and the full methodology deployed in this
 300 study are described in greater detail in section 3.3. Particular care has been taken to
 301 avoid premature convergence issues by accurately and consistently implementing both
 302 the crossover and mutation operators.

303 3.2 Random Forest

304 Random forests represent an ensemble learning method that can be used for either classi-
 305 fication or regression. In either application, random forests work by constructing several
 306 decision trees each from a subset of the training set and its features (Breiman 2001).

307 A decision tree, is a basic machine learning technique in which inputs are entered and
 308 as the decision tree is traversed, the features are binned into smaller and smaller sets
 309 allowing an output to be determined based on the given input features. From a compu-
 310 tational perspective, decision trees are generally implemented as binary trees. Where a
 311 single tree may have difficulty to accurately classify or predict an output for a complex
 312 set of inputs, the use of many trees (i.e. a forest rather than a single tree) can overcome
 313 this. The trees in a random forest each use a subset of the input features and the training
 314 set thereby reducing the biases that may result from using a single tree (James et al.
 315 2013; Hastie, Tibshirani, and Friedman 2009). The procedure of a random forest is given
 316 in algorithm 1.

317 The decision variables of the present problem include a categorical variable representing
 318 the line type of the mooring line sections and continuous variables for the lengths of the
 319 mooring lines and the anchor position. The categorical variable ($y_{l,i}$) is handled in the
 320 surrogate model using one-hot encoding wherein the categorical variable is converted
 321 to a binary string in which only one bit can be a 1. Using this encoding, there is no
 322 assumption of natural ordering of the categories which improves performance.

$$\hat{f} = \frac{1}{B} \sum_{b=1}^B f_b(x') \quad (5)$$

323 Once the forest is constructed, subsequent input data can be run through each of the
 324 decision trees. The outputs of all the trees are then averaged in order to determine the
 325 output of the forest (eq. (5)). In machine learning, an *ensemble* method is any method
 326 that uses multiple simpler machine learning techniques in its implementation. In this
 327 case, the random forest uses a series of decision trees thereby operating as an ensemble
 328 method (Olaya-Marín, Martínez-Capel, and Vezza 2013; Ahmad, Mourshed, and Yacine
 329 2017; Bagnall et al. 2016). The initial mooring designs used to train the random forest

Algorithm 1 Random Forest

Require: a training set consisting of input features (x) and output features (z), $\mathcal{S} := (x_1, z_1), \dots, (x_n, z_n)$, features \mathcal{F} , and number of trees in forest, B

for $i = 1$ to B **do**

draw a random sample \mathcal{S}^* of size n with replacement from \mathcal{S}

while minimum node size not reached **do**

randomly select f features from \mathcal{F}

select a split point among the f features

split the node into two daughter nodes

end while

add constructed tree, T_i to forest, \mathcal{A}

end for

return \mathcal{A}

330 are generated using a Monte Carlo based sampling approach. In order to increase the
 331 accuracy of the surrogate in particular to the regions being explored during the opti-
 332 mization process further mooring designs are added to the training set and the surrogate
 333 is retrained periodically in what is known as the *growing set approach* (Kourakos and
 334 Mantoglou 2009).

335 Though artificial neural networks (ANNs) currently receive much attention in the
 336 research literature, there are many problem types where a random forest (RF) is better
 337 suited. Prior to building a model, however, it is often difficult to identify which machine
 338 learning approach is best suited to a problem a priori (Olaya-Marín, Martínez-Capel,
 339 and Vezza 2013). Extending the ‘*no free lunch theorem*’ implies that though ANNs are
 340 effective for solving a particular problem does not demonstrate that they will efficiently
 341 solve all problems (Wolpert and Macready 1997; Wolpert 1995; Murphy 2012). For the
 342 present work, an RF has been deployed, as it is an effective technique for a wide range of
 343 problem types with relatively few tunable hyper parameters. This means, that from an
 344 implementation perspective, the RF is one of the easiest to set-up and get useful results
 345 from (Statnikov, Wang, and Aliferis 2008; Ahmad, Mourshed, and Yacine 2017). Though
 346 the RF has been deployed here, the modular nature of the method allows an alternate
 347 machine learning method to be implemented with minimal changes to the structure of
 348 the tool.

349 3.3 Genetic Algorithm

350 Genetic algorithms represent a family of biologically inspired population based meta-
 351 heuristic optimization algorithms that borrow ideas from natural evolution as observed
 352 in biological systems (Holland 1992). Both genetic algorithms and evolutionary algo-
 353 rithms in general operate on biological analogies based on evolution. As these types of
 354 algorithms consider a set of potential solutions each iteration rather than a single solu-
 355 tion, they are further classed as population-based. Evolutionary algorithms are commonly
 356 applied to a wide array of engineering optimization problems due to its generalized form
 357 which allows the same strategy to be applicable to a wide range of different problems.
 358 These algorithms are unable to guarantee that the true global optima is found, how-
 359 ever, they generally converge to a high quality solution in an acceptable runtime (Burke
 360 and Kendall 2013; Rao 2009; Mitchell 1998). These algorithms are therefore only imple-
 361 mented when the size of the search space or the complexity in the objective space make
 362 it infeasible to deploy traditional optimization algorithms.

363 Classical optimization strategies are generally limited to continuous, differentiable ob-
 364 jective functions. Due to their complexity, simulation based objective functions such as

365 those relating to real-world engineering optimization problems, e.g. the mooring system
 366 optimization problem, are therefore better solved by heuristics and metaheuristic algo-
 367 rithms such as the genetic algorithm (Rao 2009). Figure 3 illustrates the relationship
 368 between the time complexity of an optimization problem and the selection of the correct
 369 solution approach. As indicated in this figure, as the complexity increases, heuristics
 370 and metaheuristics become the algorithms of choice as these allow solutions to be found
 371 within acceptable timescales without requiring full enumeration.

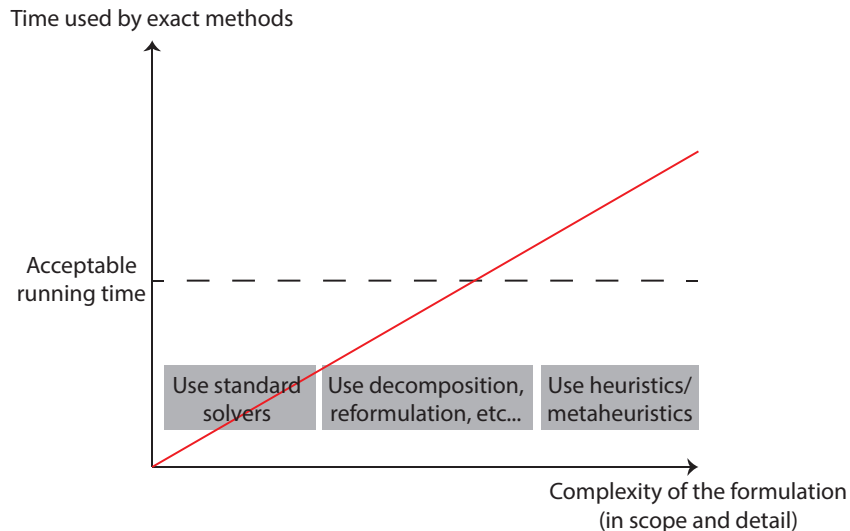


Figure 3.: Depending on the complexity of the model at hand and the time required to execute the optimization method, different algorithm types can be more appropriate to the problem.

372 In a GA, the candidate solutions within the population are formulated such that the
 373 combination of the decision variables are considered a *genome* which defines the indi-
 374 vidual solutions. In keeping with the evolutionary analogy, each solution is assigned a
 375 *fitness* by the evaluation functions with higher fitness values resulting in a higher prob-
 376 ability of contributing genetic material towards new candidate solutions. Poor solutions,
 377 as judged by the evaluation functions, are therefore assigned lower fitness scores and
 378 therefore are less likely to have traits which are passed on to the next generation. The
 379 flowchart in fig. 1 shows the steps of a GA in blue. After selecting pairs of individuals
 380 among the population to reproduce (i.e. to generate new candidate solutions), the pair
 381 undergoes what is referred to as *crossover*. During crossover, the two *parent* solutions
 382 are combined in such a way that two new solutions are generated, each with approxi-
 383 mately 50% of their genome being defined by each parent. In order to ensure that the GA
 384 does not prematurely converge to a local solution, a *mutation* operator is used to ran-
 385 domly alter the child solutions. This process is repeated until the solutions converge, or
 386 there is insufficient diversity within the remaining population for the process to continue
 387 effectively.

388 In the present implementation, a uniform crossover operator is deployed with a Gaus-
 389 sian mutation operator. Uniform crossover uses a fixed probability (50% in the present
 390 work) to determine which of the parents contributes a given gene to the child solutions.
 391 The Gaussian mutation operator uses a Gaussian distribution to alter a given gene *if*
 392 that gene is undergoing mutation (Beyer et al. 2002). Uniform crossover is selected as
 393 it ensures that the crossover process does not suffer from positional bias (Spears and
 394 Jong 1995). The Gaussian mutation operator is one of the simplest to implement, and is
 395 generally seen as a quick and effective means of applying mutation (Cazacu 2017). This

396 combination of operators which are commonly deployed in tandem, work as an effective
 397 means of ensuring that all possible solutions within the solution space are obtainable
 398 during the optimization process regardless of the initialization or the convergence of the
 399 algorithm. This helps stave off premature convergence and aids in preserving diversity
 400 within the population.

401 In multi-objective optimization, the optimizer seeks to identify a set of solutions
 402 which highlight the trade-off between the competing objectives (Deb 2001). Most multi-
 403 objective optimization approaches combine the competing objectives in such a way that
 404 the problem can be treated as a single objective problem using traditional approaches,
 405 however, in doing so much of the problem complexity and nuance is often lost. True
 406 multi-objective optimization is not simply an extension of single-objective optimization,
 407 but requires additional considerations in order to simultaneously address the various
 408 competing objectives. In a true non-trivial multi-objective optimization problem with
 409 conflicting objectives, there is not a single solution which simultaneously optimizes all
 410 of the objectives, but a Pareto front which represents the trade-off between the compet-
 411 ing objectives (see fig. 4). While an optimization algorithm applied to a single-objective
 412 optimization problem seeks to identify a single solution representing the global optima,
 413 a multi-objective optimization algorithm seeks instead to identify this Pareto front of
 414 potentially an infinite number of solutions. In the event that the objectives do not com-
 415 pete, but are rather complimentary, then a Pareto front will not be realized, as from the
 416 optimizer perspective, the problem reduces to a single objective problem.

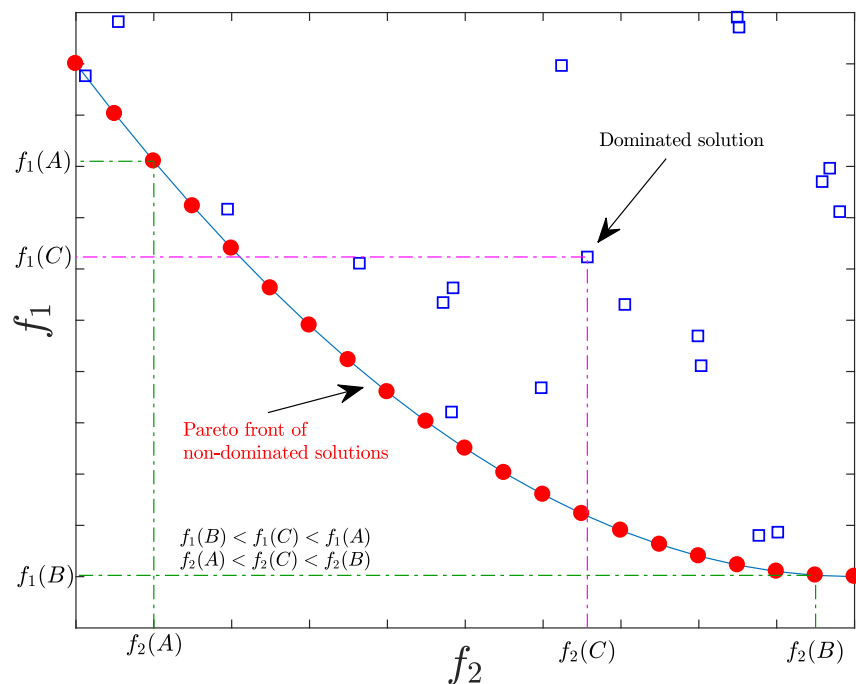


Figure 4.: Illustration of a Pareto front with dominated and non-dominated solutions for a case of two objectives both of which are to be minimized. The non-dominated solutions (red circles) are explicitly better in at least one objective and no worse in the others. For example in this figure solutions A and B lie on the Pareto front, while solution C is dominated by other solutions on the Pareto front and therefore not a member of the non-dominated set.

417 NSGA-II developed by Deb (2001); Deb and Pratap (2002) is a multi-objective genetic

418 algorithm (MOGA) which uses a sorting algorithm to identify fronts of non-dominated
 419 solutions. NSGA-II is similar to the canonical GA, but differs by using a sorting algo-
 420 rithm to identify fronts of non-dominated solutions which is combined with a diversity
 421 preservation measure referred to as the *crowding distance*. The non-dominated fronts
 422 are ranked for use in a tournament selection in which the crowding distance is used as
 423 a tie breaker in the event that the two individuals in the tournament have the same
 424 non-dominated front (Deb 2001; Deb and Pratap 2002; Burke and Kendall 2013; Brown-
 425 lee 2011). From here, standard crossover and mutation operations are used. The full
 426 NSGA-II methodology is well described in Deb and Pratap (2002) and Deb (2001). In
 427 the present implementation of NSGA-II, the parameters given in table 2 are used. In
 428 this implementation there are two crossover and mutation rates applied. The first set,
 429 those for the entire genome reflect the probability that the individual is subjected to
 430 crossover or mutation respectively while the second set, those for an individual gene (i.e.
 431 decision variable), reflect the probability, given that crossover or mutation occurs, that
 432 an individual decision variable is crossed-over or mutated.

Table 2.: Genetic Algorithm Parameters

Parameter	Value
Population Size	200
Number of Generations	50
Crossover Operator	Uniform
Mutation Operator	Gaussian
Probability of Crossover (Genome)	0.9
Probability of Crossover (Gene)	0.5
Probability of Mutation (Genome)	0.1
Probability of Mutation (Gene)	0.05
Elitism	Implicit to NSGA-II

433 The parameters used in the present implementation which are given in table 2 have
 434 been selected using a combination of recommendations from Grefenstette (1986); Deb
 435 and Pratap (2002) and from preliminary tuning of the algorithm. The current parameters
 436 are found to work well for the present problem, and as they are in line with general rules
 437 of thumb for GA parameters will likely be suitable for a wide range of problems, however,
 438 the parameters will be impacted by the specific problem at hand and should be tuned
 439 for the specific implementation of and problem instance.

440 3.4 Anomaly Detection and Retraining the Surrogate Model

441 In order to ensure that the surrogate model remains relevant to the region of the search
 442 space being explored by the optimizer, additional solutions are added to the training set
 443 (growing set approach) and the model is periodically retrained (Kourakos and Mantoglou
 444 2009; Ong, Nair, and Keane 2003). Often, retraining of surrogates is done to augment the
 445 training set with solutions in the area of interest (i.e. near the Pareto front) in order to
 446 improve the quality of solutions in this region of the search space. Alternatively, however,
 447 retraining can be done to improve the surrogate’s performance more evenly across the
 448 entire search space by using samples across the space when growing the training set. In
 449 the present work, increasing the size of the training set was done with two goals in mind:
 450 1) increasing the surrogate’s accuracy across the entire search space and 2) increasing
 451 the applicability of the surrogate by adding designs to the mooring system to ensure that
 452 the surrogate is always interpolating and not extrapolating.

453 Following each generation of the GA, the solutions estimated by the surrogate model
 454 are analysed using a local outlier factor (LOF) method which identifies potential outliers
 455 in a dataset based on a local density measure (Breunig et al. 2000; Chandola, Banerjee,
 456 and Kumar 2009). LOF is a proximity-based anomaly detection algorithm which oper-
 457 ates by comparing the local deviation of a sample with respect to its neighbours (Breunig
 458 et al. 2000). LOF operates by comparing the distance between a sample and its nearest
 459 neighbours in order to establish a density, samples which have substantially lower densi-
 460 ties than their neighbours are classed as outliers. In this case, the density is defined by a
 461 *local reachability density* (lrd) of a point. The reachability distance (d_r) and the lrd are
 462 given by eqs. (6) and (7) respectively.

$$d_r(p, o) = \max[d_k(o), d(p, o)] \quad (6)$$

$$lrd(p) = \frac{\sum_{o \in \mathcal{N}(p)} d_r(p, o)}{|\mathcal{N}(p)|} \quad (7)$$

463 These metrics are then combined to compute the LOF of a sample:

$$LOF(p) = \frac{\sum_{o \in \mathcal{N}(p)} \frac{lrd(o)}{lrd(p)}}{|\mathcal{N}(p)|} \quad (8)$$

464 where $d_k(o)$ is the distance from o to its k -th nearest neighbour, $d(p, o)$ is the true
 465 distance between p and o , $\mathcal{N}(p)$ is the set of nearest neighbours to p , d_r represents the
 466 reachability distance. LOF values of approximately 1 indicate that a sample is comparable
 467 to its neighbours while values below 1 represent inliers, and values above 1 represent the
 468 outliers.

469 Individuals which are classed as potential outliers are added to the training set and
 470 the surrogate model is retrained. In this way, as the GA proceeds, the training set from
 471 which the surrogate model is built continues to grow and covers an increasing portion
 472 of the search space. This ensures that the surrogate model is interpolating rather than
 473 extrapolating thereby reducing potential errors. Though the surrogate will still struggle
 474 with outliers, and solutions surrounding the limits of the surrogate, the use of retraining
 475 should keep these

476 Furthermore, every five generations 10% of the population is selected at random for
 477 inclusion in the training set, ensuring that not only are the extent of the model improving
 478 through the inclusion of outliers, but the surrogate also improves across the entire search
 479 space. A random subset of the population rather than those closest to the Pareto front
 480 are selected as this ensures that the surrogate has an equal probability of improving
 481 throughout the search space rather than intensifying the search only in one particular
 482 region of the space potentially leading to premature convergence to a local solution.

483 Retraining the model in this way comes at increased computational expense as ad-
 484 ditional solutions must be assessed using OrcaFlex and the training itself must also be
 485 completed at regular intervals. A preliminary sensitivity study in the development stages
 486 of this methodology found that without the retraining, the final solutions were infe-
 487 rior unless a much larger initial training set was used. The net computational cost to

488 achieve solutions of similar quality was therefore similar, however, using the retraining
 489 allowed the algorithm to adaptively select solutions to include in the training set thereby
 490 providing the maximum gain.

491 4. Case Study

492 4.1 Case Description

493 Continuing with the case study used for Pillai, Thies, and Johanning (2017, 2018b), the
 494 Offshore Code Comparison and Collaboration Continuation (OC4) semi-submersible de-
 495 signed for offshore wind turbines is modelled for deployment at Wave Hub. The OC4
 496 semi-submersible is defined in Robertson, Jonkman, and Masciola (2014) and the hydro-
 497 dynamic data is distributed as part of NREL’s FAST software package. A schematic of
 498 the OC4 semi-submersible is shown in fig. 5. The conditions at Wave Hub are defined by
 499 long term measurements in Pitt, Saulter, and Smith (2006) and shown in table 4. Using
 500 extracts from the DTOcean Database, a range of chains and polyester ropes between
 501 24 mm to 200 mm were provided to the OrcaFlex model and the optimizer (see table 3).
 502 These represent the materials and sizes likely to be deployed for offshore renewable energy
 503 applications (JRC Ocean 2016; Weller et al. 2014).

Table 3.: Available Line Types – Data from JRC Ocean (2016)

Material	Diameter [mm]	MBL [MN]	Mass [kg m ⁻¹]	Axial Stiffness [MN]	Cost [£m ⁻¹]
Chain	24	0.48	12.36	58.18	23.80
Chain	32	0.83	22.18	103.42	42.70
Chain	84	5.16	154.55	712.66	201.48
Chain	105	7.70	240.00	1113.53	312.89
Chain	152	14.43	480.00	2333.50	625.78
Chain	200	24.98	876.00	4040.00	920.11
Polyester	52	0.83	2.06	Variable	15.24
Polyester	104	3.07	7.30	Variable	54.02
Polyester	152	6.36	15.20	Variable	103.36
Polyester	192	10.10	24.08	Variable	156.52

Table 4.: Wave scatter table for Wave Hub site (Pitt, Saulter, and Smith 2006)

		Wave Period, T_z [s]				
		4	6	8	10	12
Sig. wave height, H_s [m]	6.5	-	-	9	-	-
	5.5	-	-	62	27	-
	4.5	-	9	114	27	-
	3.5	-	280	298	27	-
	2.5	96	1253	298	27	-
	1.5	1813	1945	298	35	9
	0.5	1436	693	18	-	-

504 To demonstrate the capabilities of this optimization framework, relatively small train-
 505 ing sets of 500 feasible mooring designs and approximately 2000 infeasible mooring de-

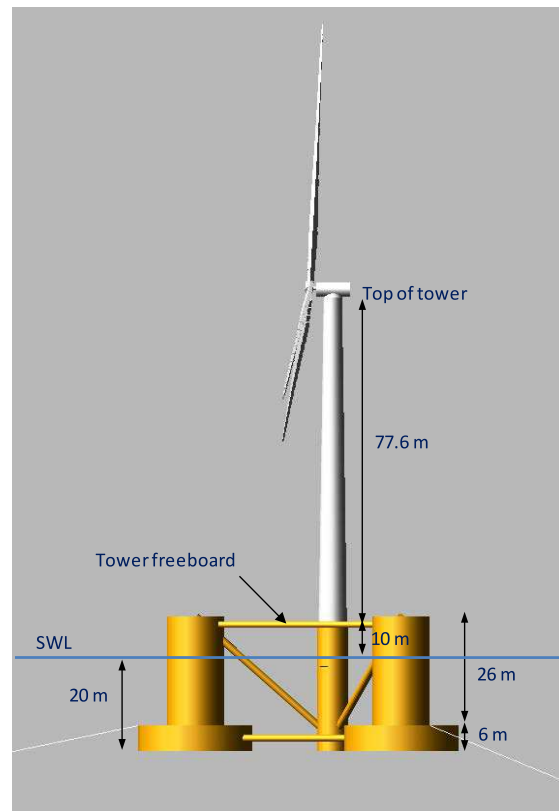


Figure 5.: DeepCwind floating wind system used as part of the Offshore Code Comparison Collaboration Continuation (OC4) project (Robertson, Jonkman, and Masciola 2014).

506 signs were used to train the classification and regression forests. Based on Oshiro, Perez,
 507 and Baranauskas (2012) the forests were designed to contain between 64 and 128 trees.
 508 A standard cross-validated grid search was deployed to determine the optimal number
 509 of trees in the forest on each occasion that the random forest was trained (Rao 2009;
 510 Müller and Guido 2016). In general, the greater the number of trees in the forest, the
 511 better the quality of the fit, however, this comes at an increase in the processing time
 512 required to construct the random forest estimator and to use the forest to estimate. Sen-
 513 sitivity studies into the number of trees in a random forest have found that for a range of
 514 problems, implementing beyond 128 trees offers diminishing returns Oshiro, Perez, and
 515 Baranauskas (2012).

516 4.2 Results

517 The final generation of feasible solutions from execution of the surrogate-model based
 518 multi-objective genetic algorithm are shown in fig. 6 with solutions of interest highlighted.
 519 These solutions of interest, the minimum cumulative fatigue damage, minimum cost,
 520 and a compromise solution are described in tables 5 to 7 respectively. Figure 7 explores
 521 the knee of this curve showing the solutions which simultaneously best minimize both
 522 solutions representing an equal priority between the two objectives.

523 Following 50 generations of the optimization, the surrogate models had classification
 524 ROC AUC of 0.862 and an outright accuracy of 0.998. The regression model had an R^2
 525 of 0.915. These results indicate that through the use of this hybrid surrogate model for
 526 constraint satisfaction and for output feature values achieves high accuracy.

527 Though metrics such as the mean averaged error (MAE) and root mean squared error

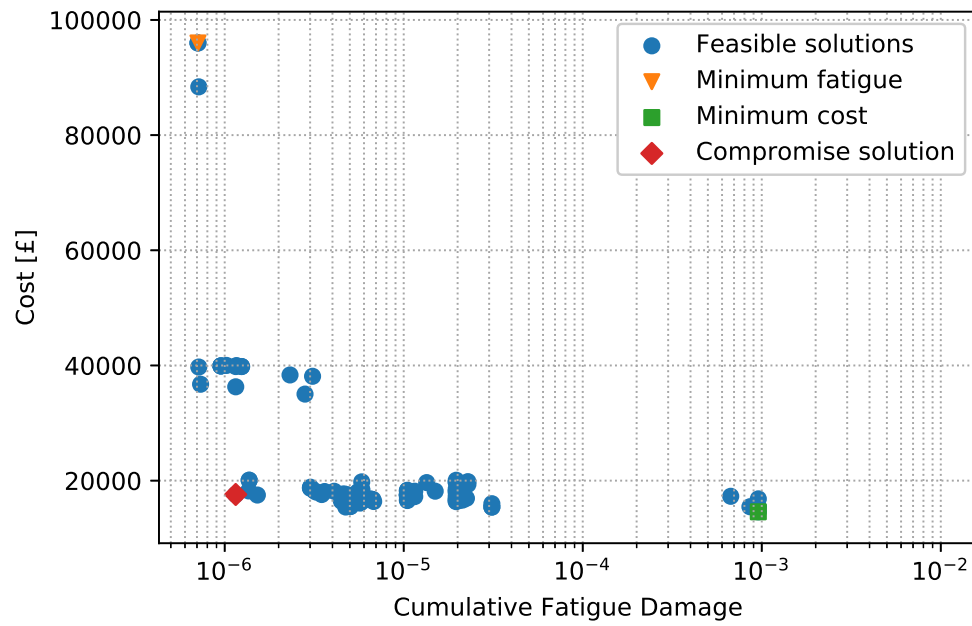


Figure 6.: Feasible solutions following final generation of optimization showing the trade-off between the mooring system cost and the cumulative fatigue damage; minimum cost and minimum fatigue solutions highlighted.

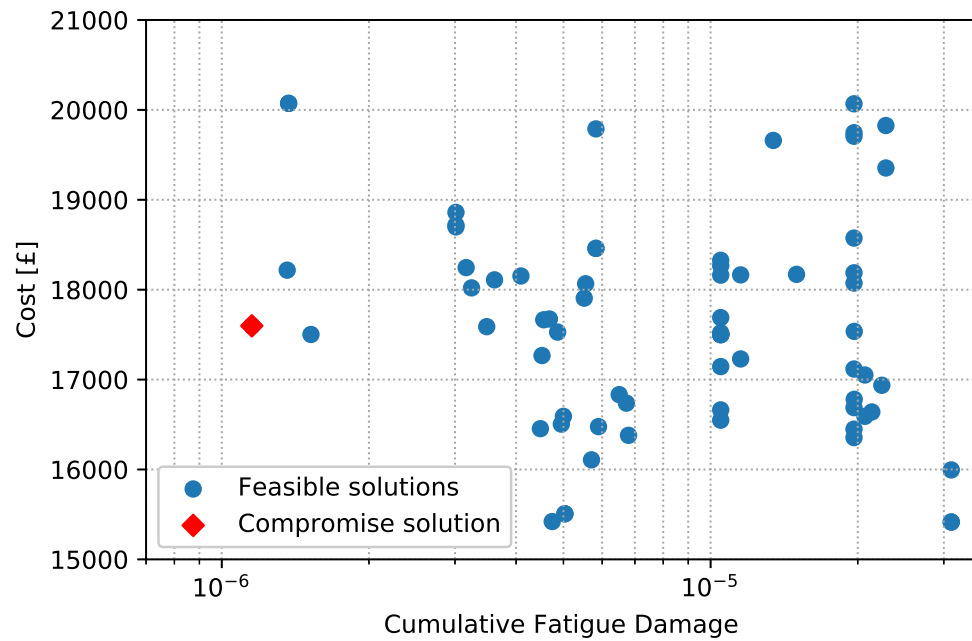


Figure 7.: Focus on solutions at the knee of the trade-off curve after the final generation of the optimization, highlighting the wide range of cost levels for any given fatigue.

528 (RMSE) are commonly used, we use the root mean square logarithmic error (RMSLE)
 529 here. The RMSLE is given by eq. (9).

Table 5.: Numerical result - minimum fatigue damage

Line	Anchor distance [m]	Anchor direction [°]	Line length [m]	Line type
1	122	242	119	192 mm polyester
1			32	32 mm chain
2	379	10	340	32 mm chain
3	358	121	338	192 mm polyester
3			17	200 mm chain

Table 6.: Numerical result - minimum cost

Line	Anchor distance [m]	Anchor direction [°]	Line length [m]	Line type
1	120	239	13	152 mm polyester
1			159	24 mm chain
2	172	353	208	24 mm chain
2			25	32 mm chain
3	200	119	254	24 mm chain

Table 7.: Numerical result - knee

Line	Anchor distance [m]	Anchor direction [°]	Line length [m]	Line type
1	183	239	18	152 mm polyester
1			212	24 mm chain
2	172	358	236	24 mm chain
3	200	135	252	24 mm chain

$$RMSLE = \sqrt{\frac{1}{n} \sum_{i=1}^n \left[\ln(h_i + 1) - \ln(\hat{h}_i + 1) \right]^2} \quad (9)$$

530 where there n samples, h_i is the true value of sample i and \hat{h}_i is the predicted value
531 of sample i using the surrogate model. The RMSLE differs from the RMSE in that the
532 RMSLE applies the natural logarithm to both the predicted and true values prior to
533 computing the root mean square error. This is done to balance the impact of both big
534 and small predictive errors. Especially given the different scales on which the output
535 features operate, it was felt that using the MAE or RMSE would cause any errors in
536 the cost estimate to dominate the error function and therefore give a biased measure
537 of the error. The RMSLE avoids this and allows the error to convey greater meaning
538 on the performance of the surrogate. Even in the event that all the output features are
539 normalized to similar scales, the RMSLE still has the advantage over the MAE and
540 RMSE in that it is not biased by the sizes of the error.

Table 8.: Surrogate Model RMSLE

Output Feature	RMSLE
Line 1 Cumulative Fatigue	0.60
Line 2 Cumulative Fatigue	2.91
Line 3 Cumulative Fatigue	1.26
Cost	1.88
Overall	1.87

541 4.3 Comparison to Direct Optimization

542 The surrogate assisted optimization methodology developed in this paper seeks to offer
 543 an improved means of optimizing the mooring designs of offshore renewable energy de-
 544 vices. In order to demonstrate the value of this approach, a comparison against direct
 545 optimization using NSGA-II has been completed.

546 The final Pareto front from executing the surrogate assisted optimization routine as
 547 described above is shown again against the results following 9 generations of direct opti-
 548 mization. Unfortunately, due to the increased computational complexity incurred when
 549 executing the direct optimization, it was not possible to execute the optimization for the
 550 same number of generations in a sensible time scale. From these results, it can be seen
 551 that in a fraction of the time (see table 9); the surrogate model can evaluate significantly
 552 more mooring systems, identifying a superior Pareto front. Furthermore, the best solu-
 553 tions with respect to the fatigue damage are an order of magnitude lower when using
 554 the surrogate assisted model as a result of the more complete optimization that can be
 555 achieved for a given computational effort. As the surrogate assisted solutions dominate
 556 the direct optimization results, with respect to aiding decision making, the surrogate
 557 assisted results will be of greater value.

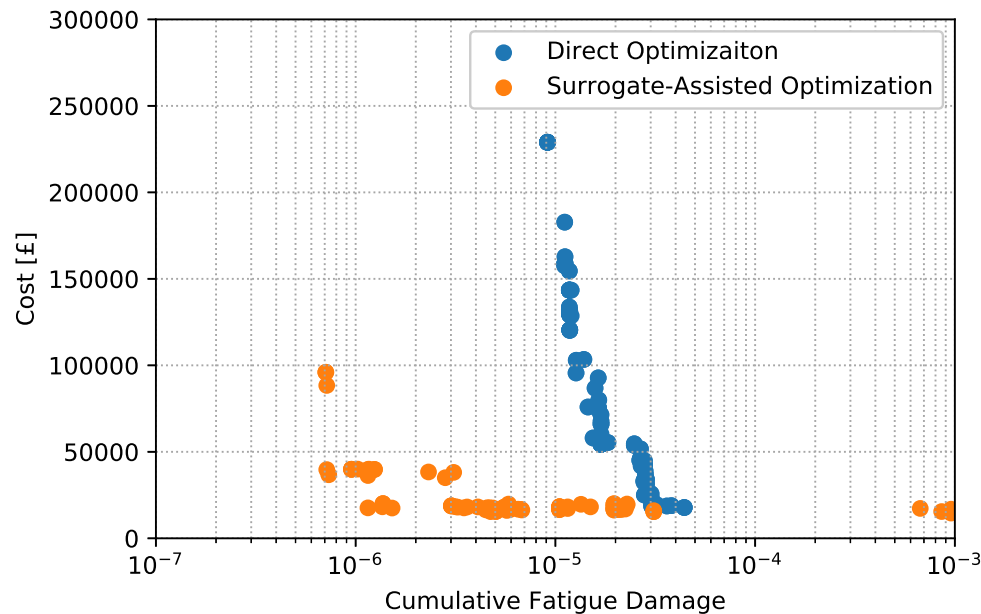


Figure 8.: Comparison of feasible solutions identified by direct optimization and surrogate assisted optimization routines.

Table 9.: Time Complexity of Surrogate Model

	Relative Time
Surrogate (No-Retraining)	1
Surrogate (With Retraining)	17
Direct Optimization	1938

558 5. Discussion

559 The presented work has detailed a new time efficient approach for the multi-objective
 560 optimization of mooring systems for renewable energy systems. This implementation of
 561 a trained random forest to replace the time-intensive time-domain simulations generally
 562 used in the design process reduces the average time required to evaluate a single mooring
 563 design (including time spent retraining the surrogate) from 692.2 s to 6.1 s running on an
 564 Intel Xeon E5440 rated at 2.83 GHz with 16 GB RAM representing a time reduction on
 565 the order of 114. This is a marked improvement over the traditional design approaches
 566 especially considering the high level of accuracy in both the classifier’s ability to identify
 567 if solutions are compliant with respect to the constraints, and the regressor’s ability to
 568 determine the cost and cumulative fatigue damage. In fact, without implementation of
 569 the surrogate assisted framework, a direct NSGA-II based optimization routine exceeds
 570 30 h in evaluating and evolving each generation of solutions while the surrogate assisted
 571 framework requires on average approximately 15 min.

572 In fig. 6, the minimum cost solution and minimum fatigue solution are both highlighted.
 573 These solutions represent the extents of the Pareto front and can be thought of as the
 574 solutions to the single objective optimization problems along either of these objectives.
 575 From the shape of the curve it is apparent that the two objectives are indeed competing,
 576 however, there are a high density of solutions near the knee of the curve that may
 577 potentially represent a good compromise solution between the two extremes. In fact,
 578 though the minimum cost solution coincides with the maximum fatigue damage solution,
 579 there are many solutions of similar cost values at significantly lower fatigue levels.

580 Figure 7 highlights the solutions of the final population located at the knee of the
 581 Pareto front. This figure shows more solutions than just the Pareto front highlighting
 582 that there is a wide range of cost levels for a given fatigue level. This is important
 583 information for a decision maker as it indicates that the overall cost of the mooring
 584 system can be changed, however, if the high fatigue lines or components are not altered,
 585 it may not impact the overall cumulative fatigue damage.

586 The result described in table 5 minimizes the fatigue loading by increasing the length
 587 of the heavily loaded line, line 2, utilizing a long catenary chain thereby reducing the
 588 fatigue damage by reducing the tension experienced relative to the MBL. Furthermore,
 589 compared to the lower cost solutions, greater lengths of polyester are used throughout
 590 the mooring system and a much larger mooring footprint is required as a result of the
 591 longer catenary moorings.

592 Exploring the other extreme, the minimization of the system’s material cost as shown
 593 in table 6 reduces the use of polyester lines in favour of chain constructions. Further-
 594 more, the mooring lines are shorter, and anchors moved closer to the platform for a
 595 smaller footprint. Though this significantly reduces the cost, the fatigue levels are also
 596 significantly increased.

597 The ‘compromise’ solution detailed in table 7 represents an attempt at trying to balance
 598 the two objectives. In this case, the knee of the curve is targeted trying to find a solution
 599 which most equally balances the two objectives. This solution similar to the low cost
 600 solution, however, makes use mooring lines in order to reduce the fatigue with limited

601 impact in cost. If the relevant mooring system designer had a different prioritization of
602 the objectives, then an alternate design from the non-dominated front would prove to be
603 more important, however, this is specific to the relative importance of the objectives to
604 the mooring system designer.

605 Though the RF has been deployed to develop the present surrogate, the present frame-
606 work can be used in future work to benchmark different machine learning algorithms for
607 this specific application allowing the most suitable surrogate to be deployed.

608 6. Conclusion

609 The results presented indicate that for the present case study, the surrogate assisted
610 optimization methodology is an effective means of mapping the design space and subse-
611 quently of optimizing the mooring system with a reduction of the time required on the
612 order of 114 times. The surrogate model can in this case accurately estimate the features
613 of interest to sufficient accuracy to provide useful information to the optimization pro-
614 cess. The use of two separate models, one for the classification of solutions as feasible or
615 infeasible had an outright accuracy of 0.998 indicating high reliability of the classifier.
616 The use of both a classifier and a regression model ensures that the regression is only
617 done for valid solutions, and the deployment of an anomaly detection algorithm helps in
618 the identification of outliers which should be added to the training set to improve the
619 performance of the surrogate. This works to orient the surrogate so that it has a relevant
620 scope for interpolation and is not forced to extrapolate predictions which has helped the
621 regression model achieve an RMSLE across all output features of 1.87.

622 The multi-objective approach implemented here does not identify a single optima for
623 the given problem, but aids in decision making by presenting the trade-off between
624 competing objectives. The results from using this methodology must then be assessed by
625 a decision maker in order to determine where along the proposed Pareto front they wish
626 to operate. The case study presented therefore only presents a series of solutions which
627 from an optimization perspective are of equal value.

628 Though a large training set is used and significant time is required to generate this
629 training set, once this information is compiled for a given device and site, the optimization
630 process simply augments to this. As a result, though there could be further improvements
631 with regards to the time efficiency of the overall procedure, the present methodology
632 does demonstrate how a random forest based surrogate model could be integrated with
633 a genetic algorithm in order to aid in the design and optimization of mooring systems
634 for floating offshore renewable energy devices.

635 Future work using this framework can directly aid in the design of mooring systems for
636 prototype devices considering deployment at test facilities such as FaBTest, WaveHub,
637 or EMEC. Furthermore it can be used to explore the impact of novel mooring line
638 materials which have been designed for offshore renewable energy applications. It should
639 also be noted, that the results presented here represent the outputs from a single run
640 in order to establish the capabilities and applicability of the developed methodology.
641 Given the reduction in computational time through the deployment of this methodology
642 it is reasonable to expect that when utilizing this methodology for real design problems
643 multiple runs or a larger population size are used in order to avoid any seeding bias of
644 both the GA and the surrogate's training set.

645 Nomenclature

646 D_c Cumulative fatigue damage

647	D_c	Cumulative fatigue damage
648	D_t	Fatigue damage during time t
649	F_s	Factor of safety
650	K	Material fatigue parameter derived from S-N or T-N curve
651	LOF	Local outlier factor
652	$MBL_{l,a}$	Minimum breaking load at position a along mooring line l
653	$N(S)$	Number of stress cycles
654	$P(s)$	Probability of occurrence of sea state s
655	S	Stress amplitudes established in the rainflow cycle count
656	T	Expected operational lifetime of the mooring system
657	α_l	The decision variables for the horizontal distance between the platform and the anchor attached to mooring line l
658		
659	β	Material fatigue parameter derived from S-N or T-N curve
660	\hat{h}_i	Estimated value of sample i
661	\mathcal{A}	The set of available line constructions
662	\mathcal{C}	The set of available chains (a subset of \mathcal{A})
663	\mathcal{G}_l	The set of nodes along mooring line l that are in contact with the seabed during the dynamic simulation
664		
665	\mathcal{L}	The set of mooring lines
666	$\mathcal{N}(p)$	Set of nearest neighbours to p
667	\mathcal{S}	The set of sea states
668	ϕ_l	Initial heading of mooring line l
669	τ_d	Simulation duration
670	θ_l	The decision variables representing the angle between the platform and the anchor attached to mooring line l
671		
672	$c(y_{l,i})$	Unit cost of a mooring line construction
673	d	True distance between two points
674	d_k	Distance to k -th nearest neighbour
675	d_r	Reachability distance
676	f_1	Cumulative fatigue damage objective function
677	f_2	Material cost objective function
678	h_i	True value of sample i
679	lrd	Local reachability distance
680	n	Number of samples
681	s	A specific sea state in set \mathcal{S}
682	$v_{l,a}$	The minimum vertical distance between position a along mooring line l and the seabed
683		
684	x_l	The decision variables relating to the section lengths in mooring line l
685	y_l	The decision variables relating to the material of each section in mooring line l
686	z	Target output features

687 Acknowledgements

688 This work is funded by the EPSRC (UK) grant for the SuperGen Marine United King-
689 dom Centre for Marine Energy Research (UKCMER) [grant number: EP/P008682/1].
690 The authors would also like to thank Jason Jonkman at NREL who provided the hydro-
691 dynamic data for the OC4 semi-submersible and Orcina Ltd. for providing OrcaFlex.

692 **References**

- 693 Ahmad, Muhammad Waseem, Monjur Mourshed, and Rezgui Yacine. 2017. “Trees vs Neu-
694 rons: Comparison between Random Forest and ANN for high-resolution prediction of build-
695 ing energy consumption Trees vs Neurons: Comparison between Random Forest and ANN
696 for high-resolution prediction of building energy consumption.” *Energy & Buildings* 147:
697 77–89. <http://dx.doi.org/doi:10.1016/j.enbuild.2017.04.038>
698 <http://dx.doi.org/10.1016/j.enbuild.2017.04.038>.
- 699 Amzallag, C., J. P. Gerey, J. L. Robert, and J. Bahuaud. 1994. “Standardization of the rainflow
700 counting method for fatigue analysis.” *International Journal of Fatigue* 16 (4): 287–293. [arXiv:
701 1011.1669v3](https://arxiv.org/abs/1011.1669v3).
- 702 Bagnall, Anthony, Jason Lines, Aaron Bostrom, and James Large. 2016. “The Great Time Se-
703 ries Classification Bake Off: An Experimental Evaluation of Recently Proposed Algorithms.
704 Extended Version.” *eprint arXiv:1602.01711* 19. 1602.0171. [http://arxiv.org/abs/1602.
705 0171](http://arxiv.org/abs/1602.0171).
- 706 Beyer, Hans-Georg, Hans-Georg Beyer, Hans-Paul Schwefel, and Hans-Paul Schwefel. 2002.
707 “Evolution strategies A comprehensive introduction.” *Natural Computing* 1 (1): 3
708 – 52. <http://www.springerlink.com/content/2311qapbrwgrcyey>
709 <http://link.springer.com/10.1023/A:1015059928466>.
- 710 Breiman, Leo. 2001. “Random Forests.” *Machine Learning* 45 (1): 5–32. [arXiv:1011.1669v3](https://arxiv.org/abs/1011.1669v3).
- 711 Breunig, Markus M., Hans-Peter Kriegel, Raymond T. Ng, and Jörg Sander. 2000. “LOF: Identifying
712 Density-Based Local Outliers.” *Proceedings of the 2000 Acm Sigmod International Con-
713 ference on Management of Data* 1–12. [http://citeseerx.ist.psu.edu/viewdoc/summary?
714 doi=10.1.1.35.8948](http://citeseerx.ist.psu.edu/viewdoc/summary?doi=10.1.1.35.8948).
- 715 Brown, D. T., and S. Mavrakos. 1999. “Comparative study on mooring line dynamic loading.”
716 *Marine Structures* 12 (3): 131–151.
- 717 Brownlee, Jason. 2011. *Clever Algorithms - Nature-Inspired Programming Recipes*. [http://www.
718 cleveralgorithms.com](http://www.cleveralgorithms.com).
- 719 Burke, Edmund K, and Graham Kendall. 2013. *Search Methodologies*. 2nd ed. Boston, MA:
720 Springer US.
- 721 Carbono, Alonso J Juvinao, Ivan F M Menezes, and Luiz Fernando Martha. 2005. “Mooring
722 Pattern Optimization using Genetic Algorithms.” *6th World Congress of Structural and Mul-
723 tidisciplinary Optimization, Rio de Janeiro, Brazil* (June): 1–9.
- 724 Cazacu, Razvan. 2017. “Comparative Study between the Improved Implementation of 3 Classic
725 Mutation Operators for Genetic Algorithms.” *Procedia Engineering* 181: 634–640.
- 726 Chandola, Varun, Arindam Banerjee, and Vipin Kumar. 2009. “Anomaly detection.” *ACM Com-
727 puting Surveys* 41 (3): 1–58. [arXiv:1011.1669v3](https://arxiv.org/abs/1011.1669v3). [http://portal.acm.org/citation.cfm?
728 doid=1541880.1541882](http://portal.acm.org/citation.cfm?doid=1541880.1541882).
- 729 Chugh, Tinkle, Yaochu Jin, Kaisa Miettinen, Jussi Hakanen, and Karthik Sindhya. 2018. “A
730 Surrogate-Assisted Reference Vector Guided Evolutionary Algorithm for Computationally Ex-
731 pensive Many-Objective Optimization.” *IEEE Transactions on Evolutionary Computation* 22
732 (1): 129–142.
- 733 da Fonesca Monteiro, Bruno, Aline Aparecida de Pina, Juliana Souza Baioco, Carl Horst Albrecht,
734 Beatriz Souza Leite Pires de Lima, and Breno Pinheiro Jacob. 2016. “Towards a methodology
735 for the optimal design of mooring systems for floating offshore platforms using evolutionary
736 algorithms.” *Marine Systems & Ocean Technology* 11 (156): 55–67.
- 737 Davidson, Josh, and John V Ringwood. 2017. “Mathematical Modelling of Mooring Systems for
738 Wave Energy ConvertersA Review.” *Energies* 10 (5): 666. [http://www.mdpi.com/1996-1073/
739 10/5/666](http://www.mdpi.com/1996-1073/10/5/666).
- 740 de Pina, Aline Aparecida, Bruno da Fonseca Monteiro, Carl Horst Albrecht, Beatriz Souza
741 Leite Pires de Lima, and Breno Pinheiro Jacob. 2016. “Artificial Neural Networks for the
742 analysis of spread-mooring configurations for floating production systems.” *Applied Ocean Re-
743 search* 59: 254–264. <http://dx.doi.org/10.1016/j.apor.2016.06.010>.
- 744 de Pina, Aloísio Carlos, Aline Aparecida de Pina, Carl Horst Albrecht, Beatriz Souza Leite Pires
745 de Lima, and Breno Pinheiro Jacob. 2013. “ANN-based surrogate models for the analysis of
746 mooring lines and risers.” *Applied Ocean Research* 41: 76–86.

- 747 Deb, Kalyanmoy. 2001. *Multi-Objective Optimization using Evolutionary Algorithms*. Chichester:
748 Wiley & Sons.
- 749 Deb, Kalyanmoy, and Amrit Pratap. 2002. "A fast and elitist multiobjective genetic algo-
750 rithm: NSGA-II." *IEEE Transactions on Evolutionary Computation* 6 (2): 182–197. <http://ieeexplore.ieee.org/xpls/abs/all.jsp?arnumber=996017>.
751
- 752 Forrester, Alexander, András Sóbester, and Andy Keane. 2008. *Engineering Design via Surrogate
753 Modelling*. 1st ed. Chichester: John Wiley & Sons, Ltd.
- 754 Forrester, Alexander I.J., and Andy J. Keane. 2009. "Recent advances in surrogate-based opti-
755 mization." *Progress in Aerospace Sciences* 45 (1-3): 50–79. 1106.2697.
- 756 Forrester, Alexander I J, András Sóbester, and Andy J Keane. 2007. "Multi-Fidelity Optimization
757 via Surrogate Modelling." *Proceedings: Mathematical, Physical and Engineering Sciences* 463
758 (2088): pp. 3251–3269. <http://www.jstor.org/stable/20209374>.
- 759 Grefenstette, John J. 1986. "Optimization of Control Parameters for Genetic Algo-
760 rithms." *IEEE Transactions on Systems, Man, and Cybernetics* SMC-16 (February):
761 122–128. [#2](http://scholar.google.com/scholar?hl=en&btnG=Search&q=intitle:Genetic+Algorithms).
762
- 763 Hastie, Trevor, Robert Tibshirani, and Jerome Friedman. 2009. *The Elements of Statistical Learn-
764 ing*. 2nd ed. New York, NY: Springer Science+Business Media.
- 765 Holland, John H. 1992. "Genetic Algorithms." *Scientific American* July: 66–72.
- 766 James, Gareth, Daniela Witten, Trevor Hastie, and Robert Tibshirani. 2013. *An Intro-
767 duction to Statistical Learning*. Vol. 103. arXiv:1011.1669v3. <http://link.springer.com/10.1007/978-1-4614-7138-7>
768 <http://linkinghub.elsevier.com/retrieve/pii/S0166531607000570>
769 <http://link.springer.com/10.1007/978-1-4614-7138-7>.
- 770 Jin, Y. 2005. "A comprehensive survey of fitness approximation in evolutionary computation."
771 *Soft Computing* 9 (1): 3–12. <http://link.springer.com/10.1007/s00500-003-0328-5>.
- 772 Jin, Yaochu. 2011. "Surrogate-assisted evolutionary computation: Recent advances and future
773 challenges." *Swarm and Evolutionary Computation* 1 (2): 61–70. <http://dx.doi.org/10.1016/j.swevo.2011.05.001>.
774
- 775 Johanning, L, G Smith, and J Wolfram. 2006. "Mooring design approach for wave energy con-
776 verters." *Proceedings of the Institution of Mechanical Engineers, Part M: Journal of En-
777 gineering for the Maritime Environment* 220 (4): 159–174. <http://dx.doi.org/10.1243/14750902JEME54>.
778
- 779 JRC Ocean. 2016. "DT Ocean Suite - DTOcean Database 1.0.0." <https://setis.ec.europa.eu/dt-ocean/download/file/fid/82>.
780
- 781 Kourakos, George, and Aristotelis Mantoglou. 2009. "Pumping optimization of coastal aquifers
782 based on evolutionary algorithms and surrogate modular neural network models." *Advances in
783 Water Resources* 32 (4): 507–521. <http://dx.doi.org/10.1016/j.advwatres.2009.01.001>.
- 784 Kwan, C T, and F J Bruen. 1991. "Mooring Line Dynamics: Comparison of Time Domain, Fre-
785 quency Domain, and Quasi-Static Analyses." *Proceedings of the 23rd Annual Offshore Tech-
786 nology Conference Houston, Texas* .
- 787 Mitchell, Melanie. 1998. *An Introduction to Genetic Algorithms*. 1st ed. Cambridge, Mass.:
788 The MIT Press. [http://www.amazon.ca/exec/obidos/redirect?tag=citeulike09-20&
789 }path=ASIN/0262631857](http://www.amazon.ca/exec/obidos/redirect?tag=citeulike09-20&path=ASIN/0262631857).
- 790 Müller, Andreas C., and Sarah Guido. 2016. *Introduction to Machine Learning with Python*.
791 Sebastopol: O'Reilly Media.
- 792 Murphy, Kevin P. 2012. *Machine Learning: A Probabilistic Perspective*. Cambridge,
793 Massachusetts: The MIT Press. [http://link.springer.com/chapter/10.1007/
794 978-94-011-3532-0#_2](http://link.springer.com/chapter/10.1007/978-94-011-3532-0#_2).
- 795 Olaya-Marín, E.J., F. Martínez-Capel, and P. Vezza. 2013. "A comparison of artificial neural
796 networks and random forests to predict native fish species richness in Mediterranean rivers."
797 *Knowledge and Management of Aquatic Ecosystems* (409): 07. [http://www.kmae-journal.
798 org/10.1051/kmae/2013052](http://www.kmae-journal.org/10.1051/kmae/2013052).
- 799 Ong, Yew S., Prasanth B. Nair, and Andrew J. Keane. 2003. "Evolutionary Optimization of
800 Computationally Expensive Problems via Surrogate Modeling." *AIAA Journal* 41 (4).
- 801 Oshiro, Thais Mayumi, Pedro Santoro Perez, and Jose Augusto Baranauskas. 2012. "How
802 Many Trees in a Random Forest?." *International Workshop on Machine Learning and Data*

- 803 *Mining in Pattern Recognition* (July): 154–168. [http://www.springerlink.com/content/
804 mm0aegv576cf8wqe/](http://www.springerlink.com/content/mm0aegv576cf8wqe/).
- 805 Pillai, Ajit C., Philipp R. Thies, and Lars Johanning. 2017. “Multi-Objective Optimization of
806 Mooring Systems for Offshore Renewable Energy.” In *Proceedings of the 12th European Wave
807 and Tidal Energy Conference, Cork, Ireland*, .
- 808 Pillai, Ajit C., Philipp R. Thies, and Lars Johanning. 2018a. “Comparing Frequency and Time
809 Domain Simulations for Geometry Optimization of a Floating Offshore Wind Turbine Mooring
810 System.” *Proceedings of the ASME 2018 International Offshore Wind Technical Conference
811 (IOWTC2018) San Francisco, USA* 1.
- 812 Pillai, Ajit C., Philipp R. Thies, and Lars Johanning. 2018b. “Development of a Multi-Objective
813 Genetic Algorithm for the Design of Offshore Renewable Energy Systems.” In *Advances
814 in Structural and Multidisciplinary Optimization (WCSMO12)*, edited by Axel Schumacher,
815 Thomas Vietor, Sierk Fiebig, Kai-Uwe Bletzinger, and Kurt Maute. 2013–2026. Cham: Springer
816 International Publishing.
- 817 Pitt, E.G., A. Saulter, and H. Smith. 2006. *The wave power climate at the Wave Hub site*. Tech.
818 Rep. November. Applied Wave Research report to SWRDA.
- 819 Rao, Singiresu S. 2009. *Engineering Optimization: Theory and Practice*. 4th ed. Hoboken, New
820 Jersey: John Wiley & Sons.
- 821 Robertson, A., J. Jonkman, and M. Masciola. 2014. “Definition of the Semisubmersible Floating
822 System for Phase II of OC4.” *Golden, CO* (September): 38. [http://www.nrel.gov/docs/
823 fy14osti/60601.pdf](http://www.nrel.gov/docs/fy14osti/60601.pdf).
- 824 Rychlik, I. 1987. “A new definition of the rainflow cycle counting method.” *International Journal
825 of Fatigue* 9 (2): 1190121.
- 826 Ryu, Sam, Arun S. Duggal, Caspar N. Heyl, and Zong Woo Geem. 2016. “Cost-Optimized FPSO
827 Mooring Design Via Harmony Search.” *Journal of Offshore Mechanics and Arctic Engineering*
828 138 (6): 061303. [http://offshoremechanics.asmedigitalcollection.asme.org/article.
829.aspx?doi=10.1115/1.4034374](http://offshoremechanics.asmedigitalcollection.asme.org/article.aspx?doi=10.1115/1.4034374).
- 830 Ryu, Sam, Caspar N. Heyl, Arun S. Duggal, and Zong Woo Geem. 2007. “Mooring Cost Op-
831 timization via Harmony Search.” *26th International Conference on Offshore Mechanics and
832 Arctic Engineering* 1–8.
- 833 Schijve, Jaap. 2009. *Fatigue of Structures and Materials*. 2nd ed. Delft: Springer Science+Business
834 Media. <http://link.springer.com/content/pdf/10.1007/0-306-48396-3.pdf>[http://
835 www.springerlink.com/index/10.1007/0-306-48396-3](http://www.springerlink.com/index/10.1007/0-306-48396-3).
- 836 Shafieefar, Mehdi, and Aidin Rezvani. 2007. “Mooring optimization of floating platforms using a
837 genetic algorithm.” *Ocean Engineering* 34 (10): 1413–1421.
- 838 Shankar Bhattacharjee, Kalyan, Hemant Kumar Singh, and Tapabrata Ray. 2016. “Multi-
839 Objective Optimization With Multiple Spatially Distributed Surrogates.” *Journal of Mechani-
840 cal Design* 138 (9): 091401. [http://mechanicaldesign.asmedigitalcollection.asme.org/
841 article.aspx?doi=10.1115/1.4034035](http://mechanicaldesign.asmedigitalcollection.asme.org/article.aspx?doi=10.1115/1.4034035).
- 842 Sidarta, Djoni E., Johyun Kyoung, Jim O’Sullivan, and Kostas F. Lambrakos. 2017. “Predic-
843 tion of offshore platform mooring line tensions using artificial neural network.” *Proceedings of
844 the ASME 2017 36th International Conference on Ocean, Offshore, and Arctic Engineering
845 (OMAE 2017) June 25-30 Trondheim, Norway* 1–11.
- 846 Spears, William M, and Kenneth A De Jong. 1995. *On the Virtues of Parameterized Uniform
847 Crossover*. Tech. rep.. Washington DC: Naval Research Lab.
- 848 Statnikov, Alexander, Lily Wang, and Constantin F. Aliferis. 2008. “A comprehensive comparison
849 of random forests and support vector machines for microarray-based cancer classification.”
850 *BMC Bioinformatics* 9: 1–10.
- 851 Thies, Philipp R., Lars Johanning, Violette Harnois, Helen C M Smith, and David N. Parish.
852 2014. “Mooring line fatigue damage evaluation for floating marine energy converters: Field mea-
853 surements and prediction.” *Renewable Energy* 63: 133–144. [http://dx.doi.org/10.1016/j.
854 renene.2013.08.050](http://dx.doi.org/10.1016/j.renene.2013.08.050).
- 855 Thomsen, Jonas, Francesco Ferri, Jens Kofoed, and Kevin Black. 2018. “Cost Optimization of
856 Mooring Solutions for Large Floating Wave Energy Converters.” *Energies* 11 (1): 159. [http://
857 www.mdpi.com/1996-1073/11/1/159](http://www.mdpi.com/1996-1073/11/1/159).
- 858 Thomsen, Jonas Bjerg, Claes Eskilsson, and Francesco Ferri. 2017. *Assessment of Available Nu-*

- 859 *merical Tools for Dynamic Mooring Analysis*. Tech. rep.. Aalborg University.
- 860 Voutchkov, I, and A J Keane. 2006. "Multi-objective optimization using surrogates." *Engineering*
- 861 *Sciences* 14 (2): 155–175. <http://eprints.soton.ac.uk/37984/>.
- 862 Weller, Sam, Jon Hardwick, Lars Johanning, Madjid Karimirad, Boris Teillant, Alex Raventos,
- 863 Stephen Banfield, et al. 2014. "A comprehensive assessment of the applicability of available and
- 864 proposed offshore mooring and foundation technologies and design tools for array applications."
- 865 68. <http://www.dtocean.eu/Deliverables-Documentation/Deliverable-4.1>.
- 866 Weller, Sam D, Philipp R Thies, Tessa Gordelier, and Lars Johanning. 2015. "Reducing Reliability
- 867 Uncertainties for Marine Renewable Energy." *Journal of Marine Science and Engineering* 3:
- 868 1349–1361.
- 869 Wolpert, Dh. 1995. "No free lunch theorems for search." *Technical Report SFI-TR-95-02-010*
- 870 1–38. [http://citeseerx.ist.psu.edu/viewdoc/download?doi=10.1.1.47.7505{\&}rep=](http://citeseerx.ist.psu.edu/viewdoc/download?doi=10.1.1.47.7505{\&}rep=rep1{\&}type=pdf)
- 871 [rep1{\&}type=pdf](http://citeseerx.ist.psu.edu/viewdoc/download?doi=10.1.1.47.7505{\&}rep=rep1{\&}type=pdf).
- 872 Wolpert, D H, and W G Macready. 1997. "No Free Lunch Theorems for Optimisation." *IEEE*
- 873 *Trans. on Evolutionary Computation* 1 (1): 67–82.
- 874 Won, Kok Sung, and Tapabrata Ray. 2005. "A framework for design optimization using surro-
- 875 gates." *Engineering Optimization* 37 (7): 685–703.